Experimental Correlations for the Performance and Aperture Selection of Wire-Wrapped Screens in Steam-Assisted Gravity Drainage Production Wells

Jesus David Montero Pallares, Chenxi Wang*, Mohammad Haftani, and **Alireza Nouri,** University of Alberta

Summary

Wire-wrapped screens (WWSs) are one of the most-commonly used devices by steam-assisted gravity drainage (SAGD) operators because of the capacity to control plugging and improve flow performance. WWSs offer high open-to-flow area (OFA) (6 to 18%) that allow a high release of fines, hence, less pore plugging and accumulation at the near-screen zone. Over the years, several criteria have been proposed for the selection of aperture sizes on the basis of different industrial contexts and laboratory experiments. Generally, existing aperture-sizing recommendations include only a single point of the particle-size distribution (PSD). Operators and academics rely on sand-control testing to evaluate the performance of sand-control devices (SCDs). Scaled laboratory testing provides a straightforward tool to understand the role of flow rate, flowing phases, fluid properties, stresses, and screen specifications on sand retention and flow impairment.

This study employs large-scale prepacked sand-retention tests (SRTs) to experimentally assess the performance of WWSs under variable single-phase and multiphase conditions. The experimental results and parametric trends are used to formulate a set of empirical equations that describe the response of the WWS. Several PSD classes with various fines content and particle size are tested to evaluate a broad range of PSDs. Operational procedures include the coinjection of gas, brine, and oil to emulate aggressive conditions during steam-breakthrough events.

The experimental investigation leads to the formulation of predictive correlations. Additional PSDs were prepared to verify the adequacy of the proposed equations. The results show that sanding modes are both flow-rate and flowing-phase dependent. Moreover, the severity or intensity of producing sand is greatly influenced by the ratio of grain size to aperture size and the ability to form stable bridges. During gas and multiphase flow, a dramatic amount of sanding was observed for wider apertures caused by high multiphase flow velocities. However, liquid stages displayed less-intense transient behaviors. Remarkably, WWSs rendered an excellent flow performance even for low-quality sands and narrow apertures. Although further and more complete testing is required, empirical correlations showed good agreement with experimental results.

Introduction

SAGD is widely implemented as the thermal method to effectively extract bitumen from Alberta's oil sands in Western Canada (Gates et al. 2007; Zhang et al. 2007). In the SAGD process, a horizontal well pair is located close to the base of the reservoir formation. The upper well injects steam into the formation to transfer latent heat and reduce the viscosity of cold bitumen. Heated oil flows along the edges of a growing steam chamber toward the lower production well (Butler 1992).

SAGD wells are equipped with SCDs to restrain the production of solid particles and support the collapse of the unconsolidated formations. **Fig. 1** shows a schematic of a SAGD well pair, steam chamber, and WWS as the SCD. The production of sand particles poses a threat for integrity damage in the tubing, artificial-lift equipment, valves, chokes, and surface facilities (Ott and Woods 2003; Han et al. 2007; Isehunwa and Farotade 2010). When inadequate SCD designs are implemented, expensive cleanout operations or liner replacements are required to recuperate effective production and unplug production tubing (Chakrabarty et al. 1998; Fattahpour et al. 2018a). Slotted liner (SL), WWSs, and punched screens are the most-commonly used SCDs in SAGD operations.

The WWS has been the preferred choice for producer wells in recent years because of the superior field-flow performances and plugging issues experienced with some SL completions caused by corrosion (Romanova and Ma 2013; Spronk et al. 2015; Williamson et al. 2016). The greater response of WWSs is attributed to their high OFAs (6 to 15%) that translate in lower pressure differentials and resistance to reach severe plugging. In fact, the WWS has been suggested to be suitable for low-quality sands in which there is a risk for thermal formation damage and severe fines migration (Romanova et al. 2015; Williamson et al. 2016). The WWS consists of a continuous profiled wire wrapped onto a base pipe. The wire jackets are usually fabricated in stainless steel to prevent corrosion. The wire spacing (aperture size) provides the retention mechanism, and the base pipe provides mechanical support to the wire jacket through ribs or rods resting over the base pipe (Fig. 1). Although the WWS has a better flow performance and higher resistance to corrosion, the cost of a WWS is higher than the SL because of the material and manufacture. Also, another disadvantage of WWSs is the relative lower mechanical integrity because of the wired structure compared with the SL (Fattahpour et al. 2018b).

The proximity between wires results in a strong aperture interaction that influences the time for achieving bridge stability (Mondal et al. 2010; Chanpura et al. 2012a). A high OFA supposes more space available for sand production, and aperture selection guidelines usually suggest narrower apertures when compared with the SL. A heuristic rule of thumb for the WWS indicates an aperture size smaller by 0.004 to 0.008 in. than the same for the SL (Fattahpour et al. 2018b).

SRT is usually implemented to evaluate and rank the performance of different SCDs. In this study, the prepacked SRT procedure is used because it represents the SAGD downhole condition more closely than slurry SRT. During the preheating stage in SAGD, the sand around the borehole comes in contact with the hot steam. Hence, the bitumen (as the bonding material) melts, resulting in the collapse of the oil sands onto the screen, creating a high-porosity zone (Guo et al. 2018).

* Corresponding author: wangchenxi_92@163.com

Original SPE manuscript received for review 15 August 2019. Revised manuscript received for review 26 September 2019. Paper (SPE 200473) peer approved 6 November 2019.

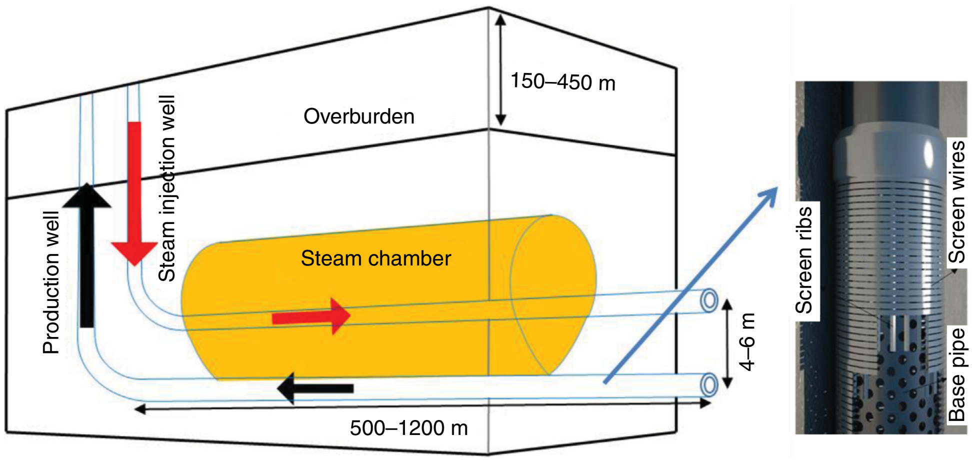

Fig. 1—Schematic of SAGD well pair and WWS completion.

In the prepacked SRT, fluid injection begins from the top of the sandpack toward the screen. Produced sand and pressure-drop readings are used for performance analyses. Experimental studies have identified the dominance of representative grain sizes on the sand-retention ability of WWSs. For instance, Gillespie at al. (2000) proposed 2 × D50 as the upper limit for WWS aperture size, and Ballard and Beare (2012) suggested aperture sizing on the D30 for conventional oil wells. D values are obtained through sieve analyses for a given PSD (McGlinchey 2005). For example, D10 means the sieve opening size that retains 10% of the particles of the sample in the sieve analysis.

Mondal et al. (2010, 2011) and Chanpura et al. (2012a, 2012b) have implemented discrete element methods modeling to evaluate the physics controlling sand retention. In their study, the PSD of samples is represented on the basis of the number of particles that can be tracked individually. Remarkably, the authors conducted extensive testing to correlate experimental and modeling results. The final model predicts the number of particles produced of particular grain size. However, the studies do not provide information about the flow performance of the screens, neither regarding the response of the screens at various flow rates.

Mondal et al. (2010) performed a dimensionless analysis and proposed an aperture-width parameter W_D that controls the sand-retention ability of a screen. The parameter relates a representative particle diameter (D_p) (D50 or D10) and the uniformity coefficient (UC) to the aperture width w

$$w_D = \frac{D_p \times \text{UC}}{w}, \quad (1)$$

where UC is defined as the ratio D40/D90. The numerical results showed relatively good agreement with experimental results, and the correlations provided a good approximation despite only accounting for two parameters (D_p and UC).

Laboratory testing provides a relatively straightforward and low-cost tool to evaluate the performance of SCDs. However, for the experimental approach introduced here, large volumes of mineral oil and commercial sands are implemented, which can result in expensive programs if extensive testing is required. This study aims to experimentally assess the performance of WWS using a large-scale prepacked SRT on several PSD classes of McMurray Formation. Based on the analyses of experimental results and trends, initial formulations are introduced to predict the response of WWSs regarding flow and sand-retention performance under laboratory conditions. The study identifies controlling grain sizes in the formation of particle bridges and the effect of production scenarios on the intensity of sand production. Particular attention is given to fines content in the evaluation of flow impairment. Additional PSDs were synthetically prepared to verify the suitability of the correlations for a broader range of PSD curves.

The subsequent sections provide details of the experimental apparatus, testing procedure, performance analysis, and the development of proposed correlations.

Experimental Investigation

The study implements a large-scale prepacked SRT to emulate the initial conditions of the near-wellbore region in SAGD wells. In the tests, the axial stress is chosen to be 60 psi to emulate the low effective-stress condition for the high-porosity zone formed by the collapsed formation sands in early SAGD. Later in SAGD life, the stress level can be increased in the near-screen zone because of the formation thermal expansion. However, low stresses are selected to replicate a worst-case scenario regarding sand production. It is reported in the literature that the amount of sand production is reduced with the increase of stress (Fattahpour et al. 2016; Guo et al. 2018).

The operational procedure involves several constant-rate stages and pressure-drop readings throughout the test. Produced sand and retained permeability of the WWS coupon and the adjacent sand are the testing objectives.

A test matrix was designed with three typical PSD classes of McMurray Formation in Canada (DC-III, DC-II, and DC-I) (Abram and Cain 2014). The PSDs incorporate coarse (DC-III—**Fig. 2a**), medium (DC-II—Fig. 2b), and fine (DC-I—Fig. 2c) sands to evaluate the response of WWSs under different flowing conditions and aperture sizes. Fig. 2 shows the three PSD classes with the respective synthetic mixtures used in the experimental testing.

Table 1 presents the main characteristics and fines content of the three PSDs that are synthetically prepared by mixing several commercial sands and fines. Mahmoudi et al. (2016a) showed that synthetic mixtures also display similar strength properties and shape factors as formation sands.

Experimental Apparatus. The SRT facility consists of five interconnected units: cell and accessories, fluids injection unit, data acquisition system, collection and backpressure units, and load frame. **Fig. 3** shows a schematic view and image of the experimental apparatus.

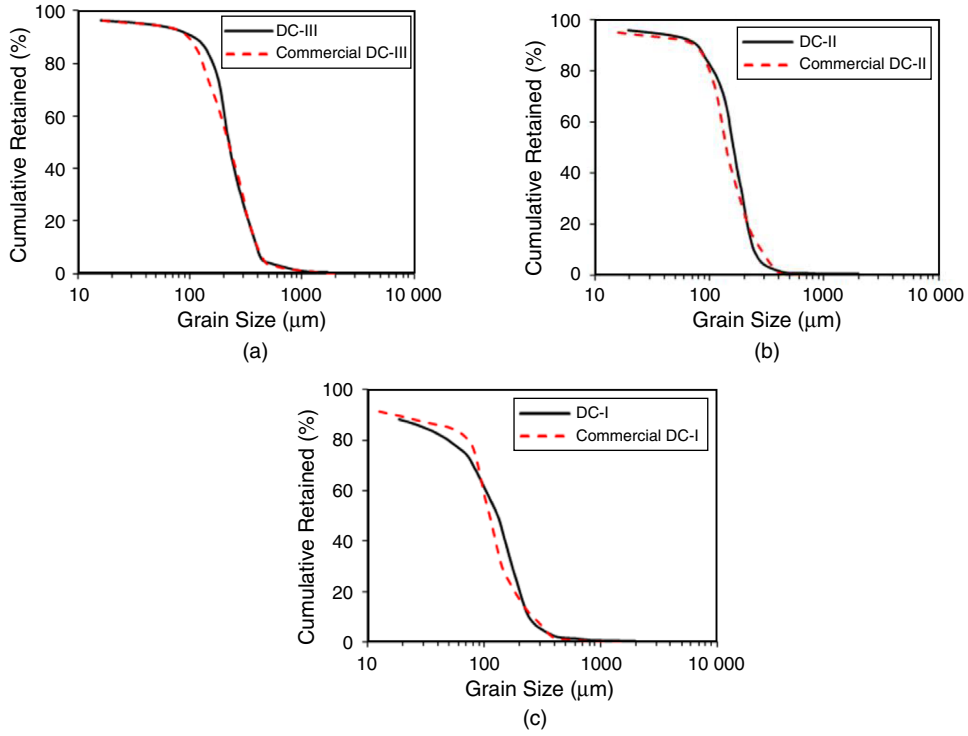

Fig. 2—PSD of formation sands and corresponding synthetic samples: (a) DC-III, (b) DC-II, and (c) DC-I.

Type of Sand	D90	D70	D50	D10	% Fines	UC	SC
DC-I	25	80	135	232	14.5	5.9	9.3
DC-II	76	118	175	260	7.4	2.7	3.4
DC-III	110	187	215	341	5.4	2.4	3.1
New PSD–1	43	92	135	657	10.7	3.5	15.3
New PSD–2	101	190	264	837	4.93	3.0	8.3

UC = D40/D90, SC = D10/D90.

Table 1—Characteristics of synthetic samples.

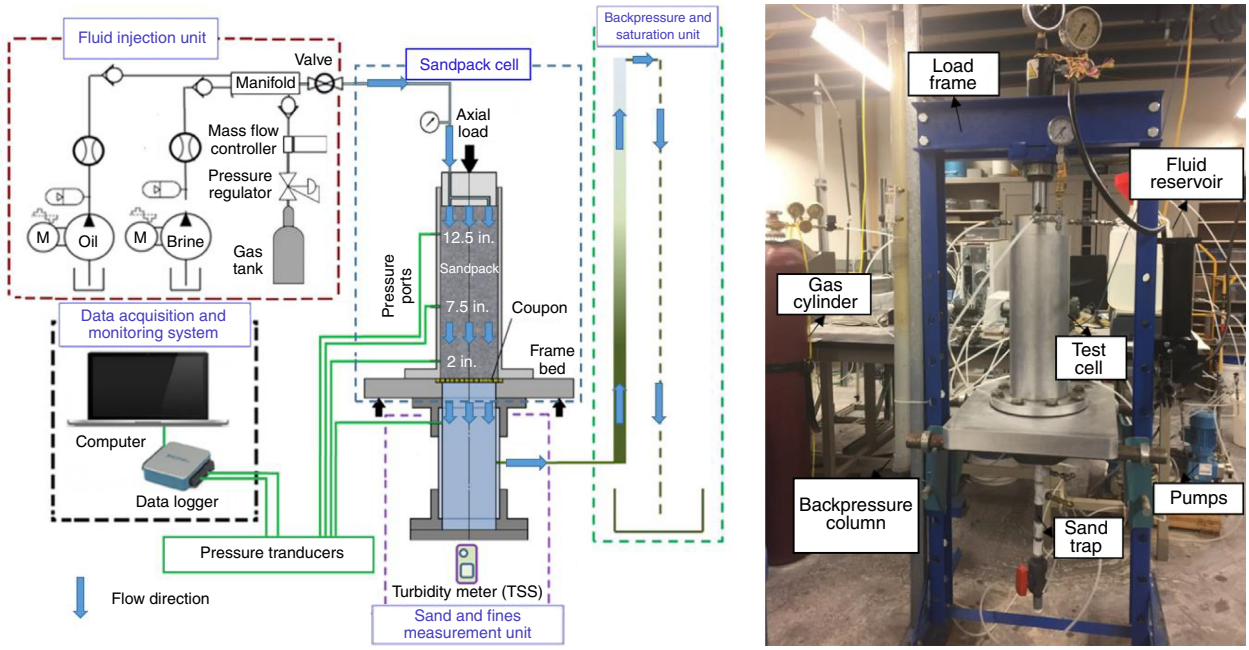

Fig. 3—Schematic and image of the prepacked SRT assembly. The location of pressure ports indicates their distance from the screen coupon.

The test cell at 47 cm in height and 15.24 cm of inner diameter is supported by a work table that separates the test cell from the sand-trap unit. In addition, the table provides sitting for the screen. Along the test cell, three connection points allow a recording of the pressure-drop evolution throughout the test. Flow-performance analyses focus at the 2 in. of the porous medium above the screen, which is regarded as the near-screen zone. The cell contains other points located 5 and 7 in. above the screen. During the test, fluids are injected from the top through the sandpack and toward the screen sample. Producing fluids with entrained particles flow inside a sand trap tube where sand particles are captured and accumulated in a compartment, and fluids go to a backpressure column.

Testing Materials and Fluid Properties. Data pertaining produced water from SAGD wells show varying levels of salinity and pH during the well life. In this study, brine is prepared to achieve 400 ppm of salinity and a pH of 7.9. From a review of the produced water properties in SAGD projects (Mahmoudi et al. 2016b), 400 ppm was found to be the lowest value from SAGD wells. Sodium chloride is used for brine preparation because Na^+ and Cl^- are the dominant ions in the produced water from SAGD wells (Cowie 2013). The use of monovalent cations, such as sodium chloride, with low salinities increases the fines mobilization potential (Khilar and Fogler 1984). Also, pH values typically range from 7.3 to 8.8, and 7.9 is selected as an average in all testing. Moreover, testing employs mineral oil of 8 cp to match bitumen conditions at high temperatures, whereas nitrogen represents the gas phase during steam-breakthrough events. The gas flow rate is measured at normal condition (20°C and 101.325 kPa).

Screens are represented by disk-shaped coupons of 6 inches in diameter **(Fig. 4)** over which the sandpack is directly deposited. The wires consist of stainless-steel material and a triangular profile with supporting rods beneath. A wide range of aperture sizes, 0.006 to 0.022 in., was implemented to integrate high-sanding and plugging-prone conditions.

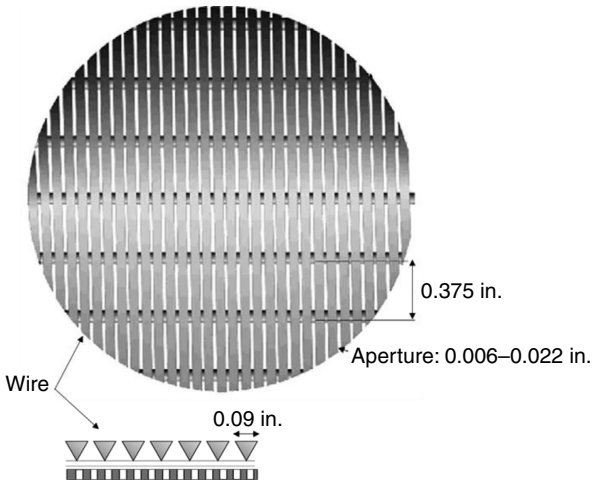

Fig. 4—Design specifications of WWS coupons (after Bakulin et al. 2008).

Testing Procedure. Commercial sands, clays, and silts are mixed at a specific proportion until achieving a uniform mixture. A sample is taken to verify the PSD and fines content of the mix. Next, 10 wt% of brine is added to the dry mixture and mixed thoroughly until achieving a uniform sample. Finally, the sand is deposited and packed layer by layer, ensuring an even porosity distribution along the sandpack, such as in the moist-tamping technique (Ladd 1978). When the packing is completed, a top platen is installed, and the load piston applies 60 psi of axial stress. Then, the sandpack sample is saturated with brine by injection from the bottom to the top at a low flow rate (250 cm^3/h) to avoid early damage of the sample and fluidization.

After the sample is fully saturated, the absolute permeability is measured by flowing brine from the top to the bottom of the sample. At this point, the three sections for pressure-differential measurements allow for checking the packing uniformity in terms of permeability. The fluid-injection program follows a progressive single-phase to two-phase flow and finally, multiphase flow **(Fig. 5).** Initially, three increasing stages of oil are injected to account for sections of the well producing high oil cuts. Then, brine and oil are injected at varying flow rates and water cuts to account for the changing conditions during SAGD production (Stahl et al. 2014). Once the maximum rate is achieved, the water cut is increased from 50 to 100%. Flow of single-phase brine represents the worst-case scenario for sand production and fines migration in which the reduction in capillary pressure reduces the resistance to particle release (Gabriel and Inamdar 1983; Wu and Tan 2001). Moreover, performance reports show that water cuts higher than 90% have been experienced in the field. Finally, brine, oil, and nitrogen are coinjected in two stages to emulate the event of steam influx. Liquid rates (oil and brine) are reduced because it is expected that the high mobility of steam restricts the liquid inflow. The duration of each flow stage was selected to ensure that each stage can successfully reach the steady-state, and the injection volume is more than one pore volume of the sample.

The flow-rate design for the tests uses a representative SAGD production rate of 4,000 bbl/d as a reference rate considering an 800-m-long liner with a 7-in. diameter. Then, three liquid-rate levels are implemented to account for different scenarios of nonuniform influx, plugging, and production ramp ups. The first two levels (2900 and 4300 cm^3/h) apply 50 and 30% of the effective flow, respectively. The maximum flow rate (7200 cm^3/h), for instance, denotes a case in which only 15% of the well contributes to the flow.

Performance Indicators and Limits

The performance of the WWS is experimentally assessed in terms of cumulative sand production and retained permeability. Retained permeability is defined as the ratio of absolute permeability at the near-screen zone measured at the last liquid stage over the initial absolute permeability (Montero Pallares et al. 2018). The near-screen zone consists of the screen plus the region within two inches above the screen. Produced sand is reported in pounds per square foot (lb/ft^2) of the coupon area to observe the sand-retention ability of the screen throughout the test under different flow conditions.

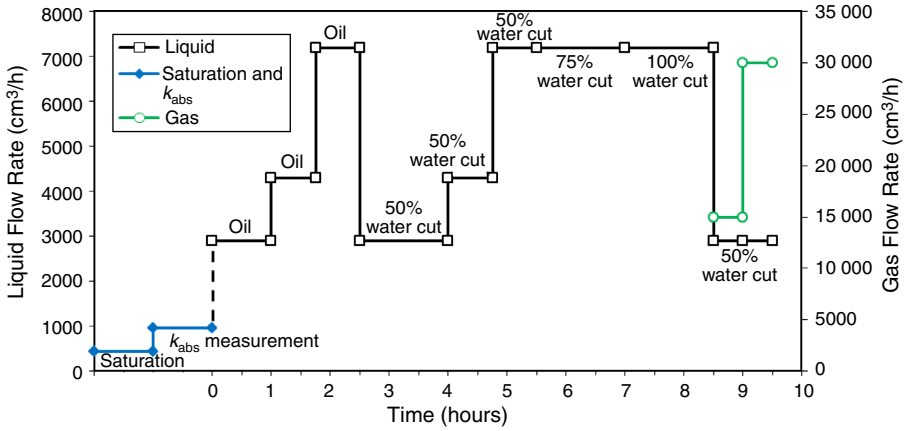

Fig. 5—Fluid injection scheme.

Sanding limits were established as unacceptable at 0.15 lb/ft^2 and moderate for 0.12 lb/ft^2. These levels correspond to a rule of thumb that the maximum amount of accumulated sand production shall be less than 1% of the liner volume in horizontal wells (Mahmoudi et al. 2018). For example, if the volume of a horizontal liner is 100 ft^3, the maximum acceptable amount of sand production will be 1 ft^3 for the entire liner. Then, this sand volume (1 ft^3) is normalized by the liner surface area, which is approximately 0.15–0.4 lb/ft^2 of sand. Likewise, Hodge et al. (2002) also suggested 0.12 lb/ft^2 as a threshold for sanding after reviewing the performance of several field deployments. In this study, produced sand of 1 lb/ft^2 in the experiments is equivalent to a total sand production of 8,800 lb for the entire horizontal liner in an 800-m well.

Separate tests were performed to determine the relative permeability of each sandpack at residual-oil saturation while preventing damage on the core. Burton and Hodge (1998) identified that 20% of screen-retained permeability as the limit to avoid production losses through analytical analyses. Later, 50% was suggested to account for additional formation damage in the near-wellbore region (Hodge et al. 2002).

Markestad et al. (1996) also proposed 50% as the minimum acceptable value for retained permeability. For this investigation, 50 and 70% are defined as the marginal and acceptable limits for retained permeability, respectively. Sanding and retained permeability limits are strongly dependent on operational conditions, artificial lifting restrictions, and specific surface-treatment practices by operators. The performance indicators in this study are expected to cover the general conditions of SAGD wells (Mahmoudi et al. 2016a).

Performance Assessment

Produced Sand. The sanding response of WWSs depends mainly on the aperture size to particle-size ratio (Constien and Skidmore 2006; Ballard and Beare 2012; Chanpura et al. 2012a) and flowing conditions (Wu and Tan 2001; Mahmoudi et al. 2016a). Therefore, the sanding level is a function of the flowing phases and velocities. **Fig. 6** presents the cumulative produced sand for the three sands for different flow stages. The produced sand is measured after each flow stage and plotted in Fig. 6. The features of the sanding responses have also been discussed by Montero Pallares et al. (2019) and are briefly covered here to facilitate the analysis. Sand-production trends show the strong effect of flowing phases. For instance, during single-phase oil injection, negligible sand production was observed even at wider apertures (Fig. 6a), and there is no significant difference between sand classes. The previous response is the result of high capillary forces increasing the bonding between grains caused by the low saturation of the wetting water phase. Substantial sand production is only observed when the wetting-phase water is mobilizing (Skjaerstein et al. 1997; Han and Dusseault 2002).

The narrowest aperture (0.006 in.) also showed negligible sanding after the onset of the brine injection during two-phase flow as seen in Figs. 6a through 6c. After the breakthrough of water production, there is no further sanding, which means sand bridges achieve sufficient stability for the testing-liquid flow rates. However, for wider apertures ($\geq$0.010 in.), the WWS displays a transient behavior with different sanding levels with the change of fluid rate and water cut. The transient behavior means varying sand production over time until stabilization. The sand production will stop after reaching the steady-state condition. At flow-rate increments, the pressure gradient through the sand bridge rises, and the drag forces exceed the frictional resistance of the bridge. Eventually, bridges achieve stability, and sand production declines and ceases. As per Figs. 6a through 6c, transient production increases as the grain size decreases, from DC-III to DC-I. This is because of the higher aperture size over the grain-size ratio, which results in weaker sand bridges.

Transient sanding also persisted during the coinjection of gas, oil, and water for most apertures, except 0.018 in. for DC-I that showed continuous sanding (Fig. 6c). Results show the dramatic effect of steam-breakthrough scenarios on sanding for wider apertures. During gas flow, high-fluid velocities and strong liquid displacement generate a high-pressure gradient at the near-screen zone. The high velocities, inadequate aperture size-to-grain ratio, and the close interaction between the apertures result in sand bridges taking a longer time to reach stability.

Figs. 7a and 7b compare the sand production before and after gas breakthrough. It is found that the total sand production after gas breakthrough is much higher than before, which means higher sanding when the flow condition changes from two phase to three phase. Both figures show an exponential increase of cumulative sanding with the increase of aperture size. The curves denote a steeper trend as the grain size decreases from DC-III to DC-I. The performance until the end of the liquid stages is considered to emulate the regular SAGD operations whereas gas-influx stages represent aggressive SAGD conditions. A steam short-circuit to producer wells is an undesired event, and operators strive to prevent its occurrence because of the risks of erosion, uneven steam chamber distribution, and low productivity (Bennion et al. 2009).

Flow Performance. The interaction of the SCD with formation sand generates additional restriction to the influx of fluids. In SAGD wells, it is essential to release fine particles and prevent plugging of slots/apertures and porous medium. High-pressure differentials between the well pair have been attributed to the accumulation of fines in the proximity of production wells (Williamson et al. 2016). Lower oil productivity is experienced because of the increase in pressure. Fines accumulate in the near-screen zone and reduce the

permeability of the porous medium. **Fig. 8** presents the retained permeability for the three sand classes as a function of the aperture width. The retained permeability increases with the aperture size because of the increase of open-flow area, which allows more fines production. For all sands, the retained permeability stayed above or between the acceptable limits (50 to 70%). Interestingly, WWSs provide acceptable flow performance even when narrower apertures are used in low-quality sands, such as DC-I (high fines content) (Fig. 8). The high OFA of WWS grants a plugging-safe characteristic because of the additional area available in case severe plugging occurs. In general, coarser sands with lower fines content show less-retained permeability reduction than finer sand with higher fines content. The higher the number of fines, the higher the chances of pore plugging.

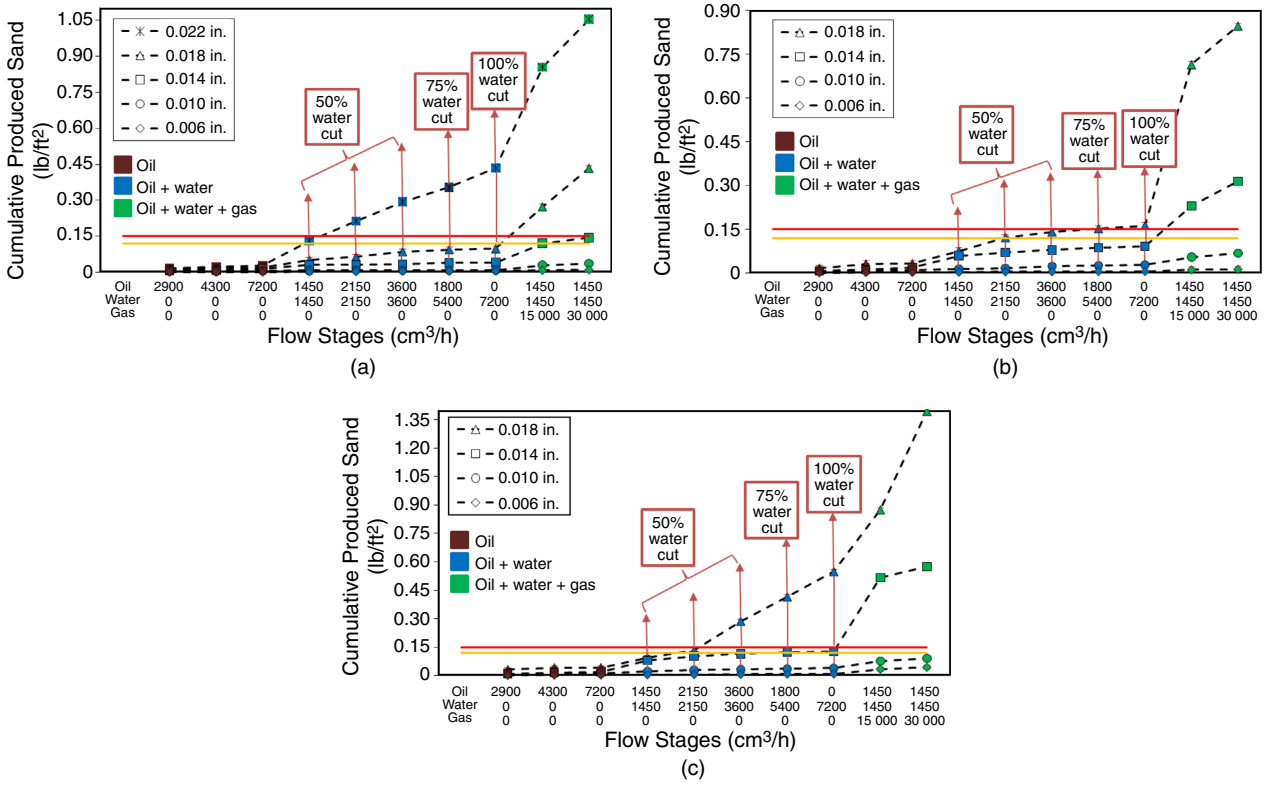

Fig. 6—Cumulative sand production for various aperture sizes at different flow stages: (a) DC-III, (b) DC-II, and (c) DC-I. Red and yellow lines represent the sanding limits of 0.15 lb/ft² and 0.12 lb/ft², respectively (after Montero Pallares et al. 2019).

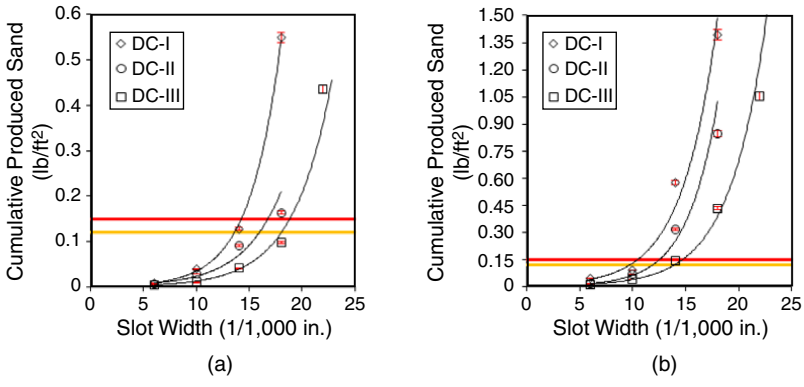

Fig. 7—Cumulative sand produced for DC-III, DC-II, and DC-I for various aperture sizes: (a) before gas breakthrough, at the end of liquid stages; and (b) after the gas breakthrough, at the end of gas-influx stages.

Performance Correlations

Large volumes of mineral oil and commercial sands are implemented in experimental studies, which can result in expensive testing programs. This section introduces formulations that predict the produced sand and retained permeability of a given PSD that undergoes an injection scheme, such as the one proposed in this research. In addition, current criteria neglect the effects of operational conditions and PSD characteristics. The formulations presented here aim to help in aperture selection in WWSs.

The procedure to generate the correlation begins with the impact analysis of each control parameter, including aperture size, fluid velocity, and PSD on produced sand and retained permeability. For instance, the produced sand results indicate an exponential function with aperture size. After examining the relationship between experimental results and different variables, a few possible structures were proposed to curve-fit the trend observed in the experiments. The coefficients were obtained through multiple iterations and regression analysis until the minimum mean absolute error was achieved. The minimum error and simple structure yield the optimal formulation structures, which we propose in this paper.

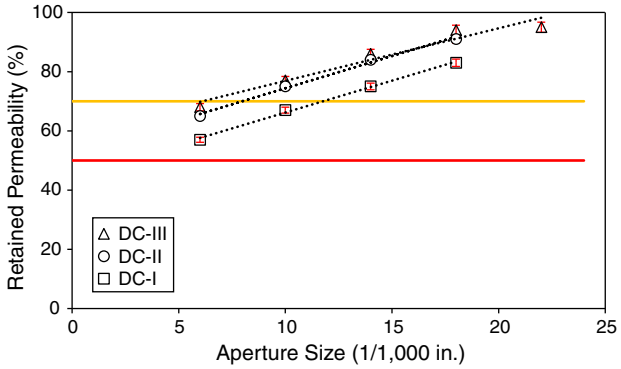

Fig. 8—Retained permeability as a function of aperture sizes. Red and yellow lines represent the retained permeability limits of 50% and 70%, respectively.

Sanding Correlation. Sand-production results were analyzed to identify the relationship between each influencing parameter and find the structure of the equation. The cumulative sand-production results showed a power function or exponential growth with the progressive change of flow rates and water cut. Logically, wider apertures and finer sands exhibit more intense trends. Gillespie et al. (2000), Constien and Skidmore (2006), Mondal et al. (2010), Ballard and Beare (2012), and Chanpura et al. (2012a) have recognized the prominence of the aperture-to-particle-size ratio on the stability of particle bridging. After examining the experimental results, a compact function structure was obtained for cumulative sand production (P_{sand})

$$P_{\text{sand}} = (52.4v_g + 45.6v_w + 1.41v_o)^{\left(\frac{2.7w}{1.34+\text{PSD}c}\right)}, \quad \ldots\ldots (2)$$

where v_g, v_w,, and v_o are the gas, water, and oil apparent velocities, respectively; w is the aperture width; and PSD_c is a parameter representing PSD. PSD_c intends to capture the features of the PSD shape that effects the production of sand and the formation of stable bridges. PSD_c is defined as

$$\text{PSD}_c = \frac{\text{D10} \times C_c}{f_c \times 100}, \quad \ldots\ldots (3)$$

where D10 represents the sieve size that retains 10% of the sample mass and f_c is the fines content. The size of fine particles is less than 44 μm. D10 provides an idea of the biggest particles in a sand mixture. C_c is known as the curvature coefficient, and it is used to classify soils regarding their gradation

$$C_c = \frac{\text{D70}^2}{\text{D40} \times \text{D90}}. \quad \ldots\ldots (4)$$

Eq. 2 shows that cumulative sand production increases with flow velocity and that a coefficient modulates the effect of each fluid phase. As observed in the experimental results, water and gas produce the most-significant effect on sand production. Therefore, their coefficients are higher than that of oil. Moreover, the produced sand growth is controlled by the aperture size to PSD coefficient ratio.

Over the years, authors have recognized the importance of the largest particles (D5, D10) in the formation of stable bridges (Coberly 1938; Suman et al. 1985; Tiffin et al. 1998; Ballard and Beare 2003; Chanpura et al. 2011). Studies by Chanpura et al. (2012b), show that particles finer than the aperture size have a negligible effect on sand bridge formation and that the shape of the coarse part of the PSD plays an essential role in sand retention. A group of large particles (D5, D10) lodge onto the aperture and retain smaller particles (McCormack 1988; Meza-Diaz et al. 2003). In other words, larger particles provide the scaffold for sand bridges by providing higher frictional forces between the grains and slot edges and improved distribution of bridging stresses (Meza-Diaz et al. 2004). The coefficient of curvature and fines content were included in the PSD variable to account for the number of smaller particles produced before stable bridges were developed. Mondal et al. (2010) showed that sorting has an effect on the production of small and fine particles.

Fig. 9a presents the agreement between the correlation and experimental results. Fig. 9b compares the results from the experiments and the correlation for each PSD. Outstanding results are obtained during liquid stages, whereas the correlation presents some differences during gas phases for wider apertures (> 0.014 in.).

The correlation introduced in this study is applicable for tests following a sequential injection, such as the one implemented here, in which the effect of a flow-rate change is carrying the cumulative effect of previous injection stages. To evaluate the influence of each variable, extensive parametric testing is required at isolated rates, phases, and PSDs.

A formulation for determining the upper bound (A_{ub}) for aperture sizing in WWSs can be obtained from the sanding correlation (Eq. 2) by setting the sanding limit at 0.12 lb/ft^2. One could apply more tolerant or strict sanding limits depending on surface-facility capabilities and the previous history of production. A_{ub} represents the wider aperture size that can maintain sanding less than the acceptable sanding thresholds (0.12 lb/ft^2). Eq. 5 provides the upper-bound aperture as a function of flow rate and PSD.

$$A_{\text{ub}} = (0.37\,\text{PSD}_C + 0.496)\frac{\ln(58.59)}{\ln(52.4v_g + 45.6v_w + 1.41v_o)}. \quad \ldots\ldots (5)$$

Retained Permeability Correlation. The trend analysis of experimental results shows a relatively linear increase of retained permeability (K_{ret}) with aperture size. The aperture size dictates the ability of the screen to release fines and control plugging (Montero Pallares et al. 2018). In addition, the slope or decay in permeability depends on the grain size; finer sands show a greater reduction in

permeability. The higher initial content of fines particles increases the risk of formation impairment (Khilar et al. 1990; Mahmoudi et al. 2017). Therefore, high relevance is given to the fines content of the sand. The empirical formulation has the following form:

$$K_{\mathrm{ret}} = 62.6 + \frac{155.54w}{1.53 + \mathrm{D10}} - 1.31f_c, \quad (6)$$

where variables are defined in the same way as in the previous section.

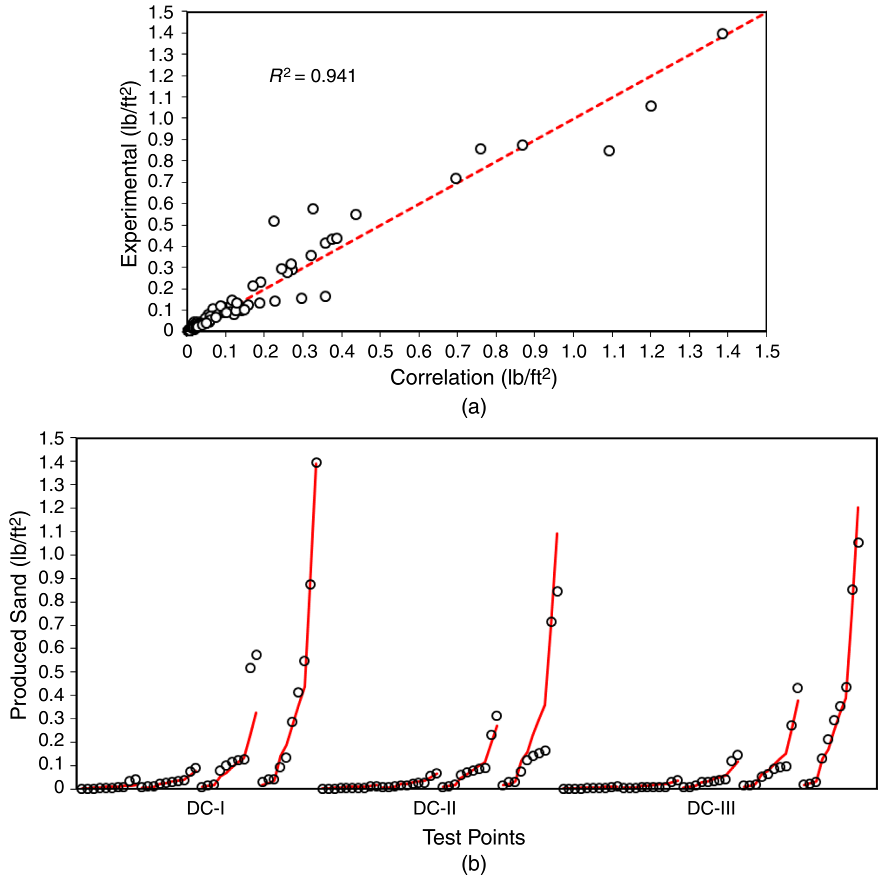

Fig. 9—Comparison of cumulative produce sand results from correlation versus experiments: (a) generalized comparison and (b) per sand class.

The D10 grain size is also included in the correlation because produced sand is always accompanied by fines. The higher the aperture-to-grain-size ratio, the higher the number of fines can be released. **Fig. 10a** shows the agreement between experimental values and results obtained from the correlation. In general, the formulation provides good results for each sand (Fig. 10b).

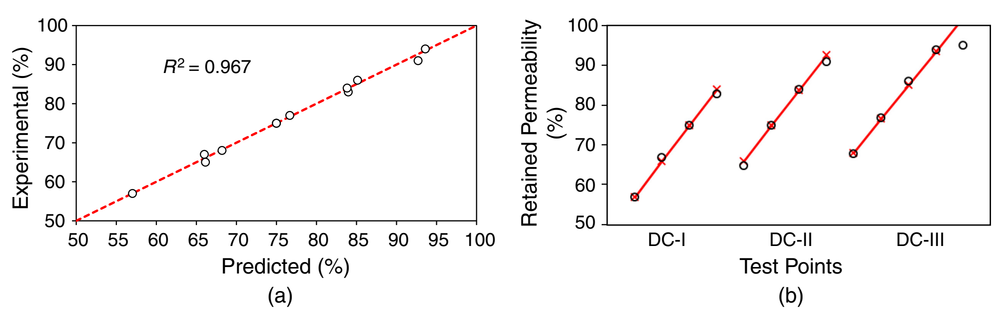

Fig. 10—Comparison of retained permeability results between experiments and correlation: (a) general comparison and (b) per sand class.

The formulation introduced in this section simplifies the evolution of formation impairment, and it does not capture the complex phenomena that control fines migration or other sources of plugging. It is a simple tool to obtain the range of retained permeabilities expected from WWS deployments depending on the formation sand and aperture widths.

The same data are used to obtain the lower bound (A_{lb}) limit for the acceptable aperture window as follows:

$$A_{\mathrm{lb}} = \left(\frac{\mathrm{D10}}{155.4} + \frac{1}{101.56}\right) \times (1.31f_c + 7.4) \quad (7)$$

The lower bound represents the narrowest aperture width that can be selected to avoid screen and formation plugging. Similar to the upper bound, A_{lb} is obtained by setting a threshold for retained permeability (70%).

Verification of Empirical Formulations

Additional tests were performed to verify the proposed correlations for different PSD shapes and characteristics. Two PSDs were synthetically prepared: a poorly sorted sand (New PSD-1) and medium-coarse sand (New PSD-2). **Fig. 11** compares these PSDs with DC sand classes.

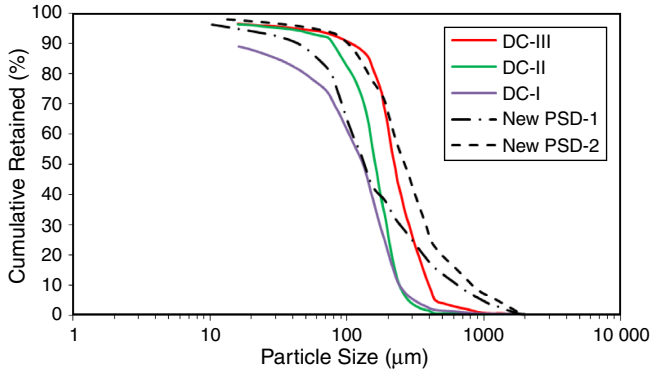

Fig. 11—New PSDs implemented for verification testing compared with DC classes.

The New PSD-1 has a large D10 grain size with a fine D50, whereas the New PSD-2 presents a better gradation. Coupons of 0.014 and 0.022 in. for aperture size were implemented to test the New PSD-1 and New PSD-2, respectively. Experimental results show a good agreement with the predicted values of the correlation **(Fig. 12a).** A maximum deviation of 18% was observed for the tests, but perceived trends are consistent with the previous testing (Fig. 12b). Remarkably, verification tests confirm the role of larger grain sizes in the development of stable bridges. Despite the large number of fine and small particles of the New PSD-1, both experimental and predicted results demonstrate that the coarse size of D10 results in low to moderate sanding.

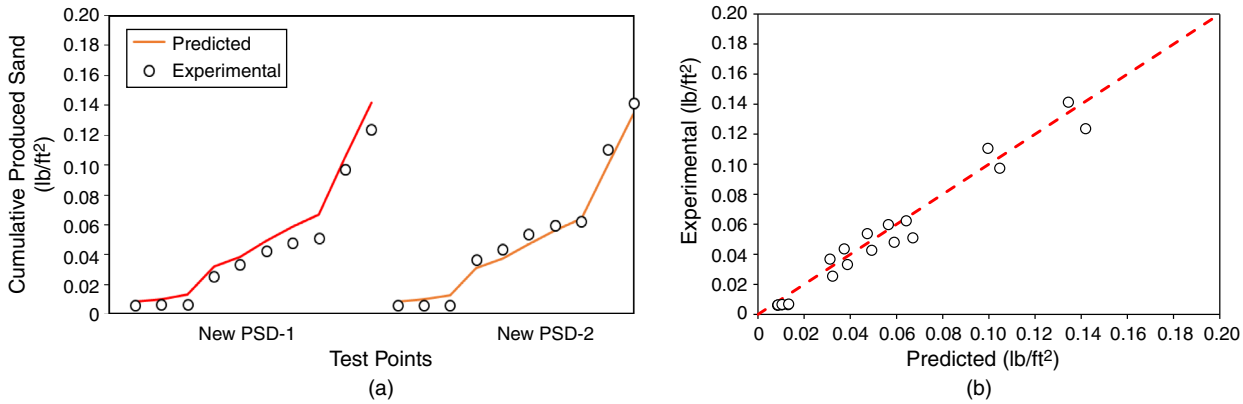

Fig. 12—Comparison predicted versus experimental cumulative produced sand for verification tests: (a) per sand class and (b) generalized comparison.

The retained permeability was calculated using the same procedure introduced in the performance-assessment section. **Table 2** compares the predicted and experimental values of retained permeability, showing a maximum deviation of 5%.

In general, the formulations provide a good predictive tool for experimental testing.

Sand Type	K_{abs} (md)	K_{rel} (fraction) at S_{or}	Predicted K_{ret} (%)	Experimental K_{ret} (%)
New PSD–1	1,570	0.47	74	78
New PSD–2	4,000	0.57	93	90

Table 2—New PSDs and verification tests for retained permeability.

Conclusions

This research introduced an SRT to study the role of operational procedures, flow rate, PSD, and screen specifications on the performance of WWSs. Results showed the dominance of the ratio particle size to aperture size on sand retention and fines production. Production scenarios strongly influence sanding intensity. Wider apertures exhibited extreme levels of production during steam-breakthrough replication stages but responded reasonably well during liquid stages. Particularly, WWSs showed excellent flow performance. A key outcome is the maintenance of retained permeability values above acceptable limits (50 to 70%), even for finer sands and narrow apertures.

In addition, performance formulations for sanding and retained permeability were elaborated on the basis of the experimental results. The correlations introduced in this study are an initial attempt to capture the overall response of WWSs. Further testing and thorough examination are needed to refine and tune an empirical formulation. The purpose of the correlation built in this study is to identify the major structure and dominant variables in the sanding and flow performance behavior of WWSs.

Note the limitations in proposed formulations. First, the oil viscosity at high temperature is assumed to be 8 cp for all reservoirs, whereas the produced liquid viscosity might vary depending on the emulsification attributes. Second, the temperature effect is only included indirectly through using an oil, which replicates the bitumen viscosity at high temperature. However, temperature might have other influences, such as accelerated clay diagenesis, asphaltene precipitation, scaling, and corrosion. Third, the clay used in experiments is kaolinite only. Swelling clay, such as smectite, is not used. More advanced testing at high pressure and high temperature is required to relegate the previously mentioned limitations.

Nomenclature

A_{lb} = lower bound for aperture window, mm
A_{ub} = upper bound for aperture window, mm
C_c = coefficient of curvature, dimensionless
D10 = sieve opening size that retains 10% of the particles in the sample, mm
D50 = sieve opening size that retains 50% of the particles in the sample, mm
D70 = sieve opening size that retains 70% of the particles in the sample, mm
D90 = sieve opening size that retains 90% of the particles in the sample, mm
D_p = representative particle diameter, μm [mm]
f_c = fines content in the sample, %
K_{abs} = absolute permeability, md
K_{rel} = relative permeability, fraction
K_{ret} = retained permeability of the near-screen zone, %
P_{sand} = cumulative produced sand, mg/cm^2
PSD_c = particle size distribution parameter, mm
SC = sorting coefficient, dimensionless
S_{or} = residual oil saturation
UC = coefficient of uniformity, dimensionless
v_g = superficial gas velocity, cm/h
v_o = superficial oil velocity, cm/h
v_w = superficial brine velocity, cm/h
w = aperture width or size, mm
W_D = dimensionless effective formation size

Acknowledgments

We would like to acknowledge that the funding for this project was provided by RGL Reservoir Management Inc. We also acknowledge the financial support provided by NSERC through their CRD program. We would like to thank Vahidoddin Fattahpour for his technical comments to improve the quality of this paper.

References

Abram, M. and Cain, G. 2014. Particle-Size Analysis for the Pike 1 Project, McMurray Formation. *J Can Pet Technol* **53** (6): 339–354. SPE-173890-PA. https://doi.org/10.2118/173890-PA.

Bakulin, A., Alexandrov, D., Sidorov, A. et al. 2008. Acoustic Waves in Sand-Screened Deepwater Completions: Comparison of Experiments and Modeling. *Geophysics* **74** (1): E45–E56. https://doi.org/10.1190/1.3002769.

Ballard, T. and Beare, S. 2003. Media Sizing for Premium Sand Screens: Dutch Twill Weaves. Paper presented at the SPE European Formation Damage Conference, The Hague, The Netherlands, 13–14 May. SPE-82244-MS. https://doi.org/10.2118/82244-MS.

Ballard, T. J. and Beare, S. P. 2012. An Investigation of Sand Retention Testing with a View to Developing Better Guidelines for Screen Selection. Paper presented at the SPE International Symposium and Exhibition on Formation Damage Control, Lafayette, Louisiana, USA, 15–17 February. SPE-151768-MS. https://doi.org/10.2118/151768-MS.

Bennion, D. B., Gupta, S., Gittins, S. et al. 2009. Protocols for Slotted Liner Design for Optimum SAGD Operation. *J Can Pet Technol* **48** (11): 21–26. SPE-130441-PA. https://doi.org/10.2118/130441-PA.

Burton, R. C. and Hodge, R. M. 1998. The Impact of Formation Damage and Completion Impairment on Horizontal Well Productivity. Paper presented at the SPE Annual Technical Conference and Exhibition, New Orleans, Louisiana, USA, 27–30 September. SPE-49097-MS. https://doi.org/10.2118/49097-MS.

Butler, R. M. 1992. Gravity Drainage to Horizontal Wells. *J Can Pet Technol* **31** (4): 31–37. PETSOC-92-04-02. https://doi.org/10.2118/92-04-02.

Chakrabarty, C., Fossey, J. P., Renard, G. et al. 1998. SAGD Process in the East Senlac Field: From Reservoir Characterization to Field Application. Paper presented at the 7th UNITAR International Conference of Heavy Crude and Tar Sands, Beijing, China, October 27–30.

Chanpura, R. A., Hodge, R. M., Andrews, J. S. et al. 2011. A Review of Screen Selection for Standalone Applications and a New Methodology. *SPE Drill & Compl* **26** (1): 84–95. SPE-127931-PA. https://doi.org/10.2118/127931-PA.

Chanpura, R. A., Mondal, S., Andrews, J. S. et al. 2012a. Modeling of Square Mesh Screens in Slurry Test Conditions for Standalone Screen Applications. Paper presented at the SPE International Symposium and Exhibition on Formation Damage Control, Lafayette, Louisiana, USA, 15–17 February. SPE-151637-MS. https://doi.org/10.2118/151637-MS.

Chanpura, R. A., Mondal, S., Sharma, M. M. et al. 2012b. Unraveling the Myths in Selection of Standalone Screens and a New Methodology for Sand Control Applications. Paper presented at the SPE Annual Technical Conference and Exhibition, San Antonio, Texas, USA, 8–10 October. SPE-158922-MS. https://doi.org/10.2118/158922-MS.

Coberly, C. J. 1938. Selection of Screen Openings for Unconsolidated Sands. Paper presented at the Drilling and Production Practice, New York, New York, USA, 1 January. API-37-189.

Constien, V. G. and Skidmore, V. 2006. Standalone Screen Selection Using Performance Mastercurves. Paper presented at the SPE International Symposium and Exhibition on Formation Damage Control, Lafayette, Louisiana, USA, 15–17 February. SPE-98363-MS. https://doi.org/10.2118/98363-MS.

Cowie, B. R. 2013. *Stable Isotope and Geochemical Investigation into the Hydrogeology and Biogeochemistry of Oil Sands Reservoir Systems in Northeastern Alberta, Canada*. Doctoral thesis, University of Calgary, Calgary, Alberta, Canada (September 2013).

Fattahpour, V., Azadbakht, S., Mahmoudi, M. et al. 2016. Effect of Near Wellbore Effective Stress on the Performance of Slotted Liner Completions in SAGD Operations. Paper presented at the SPE Thermal Well Integrity and Design Symposium, Banff, Alberta, Canada, 28 November–1 December. SPE-182507-MS. https://doi.org/10.2118/182507-MS.

Fattahpour, V., Mahmoudi, M., Roostaei, M. et al. 2018a. An Experimental Investigation into the Sand Control and Flow Performance of the Remedial Tubing Deployed Scab Liners in Thermal Production. Paper presented at the SPE Thermal Well Integrity and Design Symposium, Banff, Alberta, Canada, 27–29 November. SPE-193366-MS. https://doi.org/10.2118/193366-MS.

Fattahpour, V., Mahmoudi, M., Wang, C. et al. 2018b. Comparative Study on the Performance of Different Stand-Alone Sand Control Screens in Thermal Wells. Paper presented at the SPE International Conference and Exhibition on Formation Damage Control, Lafayette, Louisiana, USA, 7–9 February. SPE-189539-MS. https://doi.org/10.2118/189539-MS.

Gabriel, G. A. and Inamdar, G. R. 1983. An Experimental Investigation of Fines Migration in Porous Media. Paper presented at the SPE Annual Technical Conference and Exhibition, San Francisco, California, USA, 5–8 October. SPE-12168-MS. https://doi.org/10.2118/12168-MS.

Gates, I. D., Kenny, J., Hernandez, I. L. et al. 2007. Steam Injection Strategy and Energetics of Steam-Assisted Gravity Drainage. *SPE Res Eval & Eng* **10** (1): 19–34. SPE-97742-PA. https://doi.org/10.2118/97742-PA.

Gillespie, G., Deem, C. K., and Malbrel, C. 2000. Screen Selection for Sand Control Based on Laboratory Tests. Paper presented at the SPE Asia Pacific Oil and Gas Conference and Exhibition, Brisbane, Australia, 16–18 October. SPE-64398-MS. https://doi.org/10.2118/64398-MS.

Guo, Y., Roostaei, M., Nouri, A. et al. 2018. Effect of Stress Build-Up around Standalone Screens on the Screen Performance in SAGD Wells. *J Pet Sci Eng* **171:** 325–339. https://doi.org/10.1016/j.petrol.2018.07.040.

Han, D.-H., Yao, Q., and Zhao, H.-Z. 2007. Complex Properties of Heavy Oil Sand. Paper presented at the SEG Annual Meeting, San Antonio, Texas, USA, 23–28 September. SEG-2007-1609.

Han, G. and Dusseault, M. B. 2002. Quantitative Analysis of Mechanisms for Water-Related Sand Production. Paper presented at the SPE International Symposium and Exhibition on Formation Damage Control, Lafayette, Louisiana, USA, 20–21 February. SPE-73737-MS. https://doi.org/10.2118/73737-MS.

Hodge, R. M., Burton, R. C., Constien, V. G. et al. 2002. An Evaluation Method for Screen-Only and Gravel-Pack Completions. Paper presented at the International Symposium and Exhibition on Formation Damage Control, Lafayette, Louisiana, USA, 20–21 February. SPE-73772-MS. https://doi.org/10.2118/73772-MS.

Isehunwa, O. S. and Farotade, A. 2010. Sand Failure Mechanism and Sanding Parameters in Niger Delta Oil Reservoirs. *Int J Eng Sci Technol* **2** (5): 777–782.

Khilar, K. C. and Fogler, H. S. 1984. The Existence of a Critical Salt Concentration for Particle Release. *J Colloid Interface Sci* **101** (1): 214–224. https://doi.org/10.1016/0021-9797(84)90021-3.

Khilar, K. C., Vaidya, N., and Folger, H. S. 1990. Colloidally-Induced Fines Release in Porous Media. *J Pet Sci Eng* **4** (3): 213–221. https://doi.org/10.1016/0920-4105(90)90011-Q.

Ladd, R. S. 1978. Preparing Test Specimens Using Undercompaction. *Geotech Test J* **1** (1): 16–23. https://doi.org/10.1520/GTJ10364J.

Mahmoudi, M., Fattahpour, V., Nouri, A. et al. 2016a. Investigation into the Use of Commercial Sands and Fines to Replicate Oil Sands for Large-Scale Sand Control Testing. Paper presented at the SPE Thermal Well Integrity and Design Symposium, Banff, Alberta, Canada, 28 November–1 December. SPE-182517-MS. https://doi.org/10.2118/182517-MS.

Mahmoudi, M., Fattahpour, V., Nouri, A. et al. 2016b. An Experimental Investigation of the Effect of pH and Salinity on Sand Control Performance for Heavy Oil Thermal Production. Paper presented at the SPE Canada Heavy Oil Technical Conference, Calgary, Alberta, Canada, 7–9 June. SPE-180756-MS. https://doi.org/10.2118/180756-MS.

Mahmoudi, M., Fattahpour, V., Nouri, A. et al. 2017. An Experimental Evaluation of Pore Plugging and Permeability Reduction Near SAGD Sand Control Liners. Paper presented at the SPE Canada Heavy Oil Technical Conference, Calgary, Alberta, Canada, 15–16 February. SPE-184999-MS. https://doi.org/10.2118/184999-MS.

Mahmoudi, M., Fattahpour, V., Velayati, A. et al. 2018. Risk Assessment in Sand Control Selection: Introducing a Traffic Light System in Stand-Alone Screen Selection. Paper presented at the SPE International Heavy Oil Conference and Exhibition, Kuwait City, Kuwait, 10–12 December. SPE-193697-MS. https://doi.org/10.2118/193697-MS.

Markestad, P., Christie, O., Espedal, A. et al. 1996. Selection of Screen Slot Width to Prevent Plugging and Sand Production. Paper presented at the SPE Formation Damage Control Symposium, Lafayette, Louisiana, USA, 14–15 February. SPE-31087-MS. https://doi.org/10.2118/31087-MS.

McCormack, M. E. 1988. Mechanisms of Sand Retainment by Wire Wrapped Screens. Paper presented at the 4th UNITAR/UNDP Conference on Heavy Crude and Tar Sands, Edmonton, Alberta, Canada, 7–12 August.

McGlinchey, D. ed. 2005. *Characterization of Bulk Solids*. Oxford, England, UK: Blackwell Publishing Ltd.

Meza-Diaz, B., Tremblay, B., and Doan, Q. 2003. Mechanisms of Sand Production through Horizontal Well Slots in Primary Production. *J Can Pet Technol* **42** (10): 36–46. PETSOC-03-10-04. https://doi.org/10.2118/03-10-04.

Meza-Diaz, B., Tremblay, B., and Doan, Q. 2004. Visualization of Sand Structures Surrounding a Horizontal Well Slot During Cold Production. *J Can Pet Technol* **43** (12): 39–48. PETSOC-04-12-02. https://doi.org/10.2118/04-12-02.

Mondal, S., Sharma, M. M., Chanpura, R. A. et al. 2010. Numerical Simulations of Screen Performance in Standalone Screen Applications for Sand Control. Paper presented at the SPE Annual Technical Conference and Exhibition, Florence, Italy, 19–22 September. SPE-134326-MS. https://doi.org/10.2118/134326-MS.

Mondal, S., Sharma, M. M., Hodge, R. M. et al. 2011. A New Method for the Design and Selection of Premium/Woven Sand Screens. Paper presented at the SPE Annual Technical Conference and Exhibition, Denver, Colorado, USA, 30 October–2 November. SPE-146656-MS. https://doi.org/10.2118/146656-MS.

Montero Pallares, J. D., Wang, C., Haftani, M. et al. 2018. Experimental Assessment of Wire-Wrapped Screens Performance in SAGD Production Wells. Paper presented at the SPE Thermal Well Integrity and Design Symposium, Banff, Alberta, Canada, 27–29 November. SPE-193375-MS. https://doi.org/10.2118/193375-MS.

Montero Pallares, J. D., Wang, C., Nouri, A. et al. 2019. Assessment of Existing Design Criteria for Wire-Wrapped Screens in Thermal Wells. Paper presented at the 53rd US Rock Mechanics/Geomechanics Symposium, New York City, New York, USA, 23–26 June. ARMA-2019-1561.

Ott, W. K. and Woods, J. D. 2003. *Modern Sandface Completion Practices Handbook*, second edition. Houston, Texas, USA: World Oil Magazine.

Romanova, U. and Ma, T. 2013. An Investigation on the Plugging Mechanisms in a Slotted Liner from the Steam Assisted Gravity Operations. Paper presented at the SPE European Formation Damage Conference & Exhibition, Noordwijk, The Netherlands, 5–7 June. SPE-165111-MS. https://doi.org/10.2118/165111-MS.

Romanova, U., Ma, T., Piwowar, M. et al. 2015. Thermal Formation Damage and Relative Permeability of Oil Sands of the Lower Cretaceous Formations in Western Canada. Paper presented at the SPE Canada Heavy Oil Technical Conference, Calgary, Alberta, Canada, 9–11 June. SPE-174449-MS. https://doi.org/10.2118/174449-MS.

Skjaerstein, A., Tronvoll, J., Santarelli, F. et al. 1997. Effect of Water Breakthrough on Sand Production: Experimental and Field Evidence. Paper presented at the SPE Annual Technical Conference and Exhibition, San Antonio, Texas, USA, 5–8 October. SPE-38806-MS. https://doi.org/10.2118/38806-MS.

Spronk, E. M., Doan, L. T., Matsuno, Y. et al. 2015. SAGD Liner Evaluation and Liner Test Design for JACOS Hangingstone SAGD Development. Paper presented at the SPE Canada Heavy Oil Technical Conference, Calgary, Alberta, Canada, 9–11 June. SPE-174503-MS. https://doi.org/10.2118/174503-MS.

Stahl, R. M., Smith, J. D., Hobbs, S. et al. 2014. Application of Intelligent Well Technology to a SAGD Producer: Firebag Field Trial. Paper presented at the SPE Heavy Oil Conference-Canada, Calgary, Alberta, Canada, 10–12 June. SPE-170153-MS. https://doi.org/10.2118/170153-MS.

Suman, G., Ellis, R., and Snyder, R. 1985. *Sand Control Handbook*. Houston, Texas, USA: Gulf Publishing Company.

Tiffin, D. L., King, G. E., Larese, R. E. et al. 1998. New Criteria for Gravel and Screen Selection for Sand Control. Paper presented at the SPE Formation Damage Control Conference, Lafayette, Louisiana, USA, 18–19 February. SPE-39437-MS. https://doi.org/10.2118/39437-MS.

Williamson, H., Babaganov, A., and Romanova, U. 2016. Unlocking Potential of the Lower Grand Rapids Formation, Western Canada: The Role of Sand Control and Operational Practices in SAGD Performance. Paper presented at the SPE Canada Heavy Oil Technical Conference, Calgary, Alberta, Canada, 7–9 June. SPE-180700-MS. https://doi.org/10.2118/180700-MS.

Wu, B. and Tan, C. P. 2001. Effect of Water-Cut on Sandstone Strength and Implications in Sand Production Prediction. Paper presented at the DC Rocks, The 38th US Symposium on Rock Mechanics (USRMS), Washington, DC, USA, 7–10 July. ARMA-01-0027.

Zhang, W., Youn, S., and Doan, Q. T. 2007. Understanding Reservoir Architectures and Steam-Chamber Growth at Christina Lake, Alberta, by Using 4D Seismic and Crosswell Seismic Imaging. *SPE Res Eval & Eng* **10** (5): 446–452. SPE-97808-PA. https://doi.org/10.2118/97808-PA.

SI Metric Conversion Factors

$1\ \text{cp} = 10^{-3}\ \text{Pa·s}$
$1\ \text{in.} = 2.54\ \text{cm}$
$1\text{ft} = 0.3048\ \text{m}$
$1\ \text{lb} = 453.592\ \text{g}$
$1\ \text{psi} = 6894.76\ \text{Pa}$